Self-Organized Meso- and Hybridic Phases of Poly(aspartic acid) and Poly(glutamic amino acid) with Cationic Surfactants (C_nTAB, $n = 14, 16$) and a Silica Source (TEOS)

Eleftheria K. Kodona, Charalambos Alexopoulos, Eugenia Panou, and Philippos J. Pomonis*

Department of Chemistry, University of Ioannina, Ioannina 45110, Greece

Received December 5, 2006. Revised Manuscript Received January 31, 2007

In this work the self-organized mesophases obtained by the ionic interaction of poly(amino acids) poly(L-aspartic acid (P-L-Asp) and poly(L-glutamic acid) (P-L-Glu) with the cationic surfactants $C_{14}TAB$ and $C_{16}TAB$, as well as the mesoporous silicate materials obtained by addition and hydrolysis of tetraethyl orthosilicate (TEOS) on the hybridic mesophases, are described. The mesophases isolated at pH 6.5−8.5 were examined by X-ray diffraction (XRD) analysis for their structure, thermogravimetry for their thermal stability, scanning electron microscopy for their structural features, and circular dichroism (CD) for the conformation of the polypeptide−C_nTAB ($n = 14, 16$) complexes. The mesophases P-L-Asp/$C_{14}TAB$ isolated at pH 7.5 and 8.5 showed in XRD a single peak at $d = 3.45$ nm and $d = 3.54$ nm, respectively, corresponding to typical hexagonal packing of the micellar aggregates. The mesophases P-L-Asp/C_{16}-TAB isolated at pH 7.5 showed an XRD peak at $d = 3.90$ nm, corresponding to a similar hexagonal packing of larger micellar aggregates and also two peaks at $d = 3.37$ nm and $d = 1.69$ nm indicating a layered configuration of the micellar sheets. The layered component decreases by the increase of pH from 7.5 to 8.5 or the addition of small amounts (0.5%) of EtOH. The P-L-Glu/$C_{14}TAB$ mesophases isolated at pH 7.5 and 8.5 showed a single XRD peak at $d = 3.60$ nm, while the P-L-Glu/$C_{16}TAB$ system showed also a single XRD peak at $d = 4.10$ nm. The CD spectra showed that the complexes P-L-Asp/$C_{14}TAB$ possess a more random configuration compared to the P-L-Glu/$C_{14}TAB$, which have the tendency to form α- and 3_{10}-helices. The mesoporous silicate materials obtained from the systems P-L-Asp/C_{16}-TAB/TEOS and P-L-Glu/$C_{16}TAB$/TEOS showed a single XRD peak corresponding to hexagonal pore arrangement typical in MCM-41 materials. The nitrogen adsorption−desorption isotherms of the silicate mesostructures indicate that they possess high surface areas in the range 500−800 $m^2\ g^{-1}$ for the P-L-Asp/C_nTAB/TEOS and 1000−1070 $m^2\ g^{-1}$ for the P-L-Glu/C_nTAB/TEOS and ordered or semi-ordered porosity depending on the hybridic system used for isolating the corresponding mesophases.

1. Introduction

The interaction of polyelectrolytes with surfactant molecules is known to lead to self-assembled three-dimensional structures in aqueous solutions.[1−3] The first relevant studies mainly referred to pure poly(styrene sulfonate)[4,5] while the same system, complexated with surfactants, was studied later by Antonietti et al.[6,7] for potential use as novel hybridic material. The same group recognized that poly(acrylic acid) (Pac) can be complexated with cationic surfactants *N*-cetyl-*N*,*N*,*N*-trimethylammonium bromide (C_nTAB) to form mesophases with interesting polymeric properties.[8,9] In that case, the polyelectrolyte acts as a backbone of the structure, while the bounded C_nTAB species are extended outward forming some kind of micellar aggregates. Consequently, Pantazis et al.[10−12] recognized that the system Pac-C_nTAB can be employed as substrate for the development of ordered mesoporous materials like MCM-41 and SBA, either in pure silicate form or doped with oxidic species like CuOx, CeOy, and CoOz. The system Pac-C_nTAB offers the following advantages over previous methods for preparation of ordered MCM-41,[13,14] MCM-48,[15,16] and SBA[17,18] materials: (i) The

* Corresponding author. Tel.: +302651098350. Fax+302651098795. E-mail: ppomonis@cc.uoi.gr.

(1) Hayagawa, K.; Kwak, J. C. T. *J. Phys. Chem.* **1982**, *86*, 3866; **1983**, *87*, 506.
(2) Hayagawa, K.; Santerre, J. P.; Kwak, J. C. T. *Macromolecules* **1983**, *16*, 1642.
(3) Goddard, E. D. *Colloids Surf.* **1986**, *19*, 301.
(4) Shimomura, M.; Kunitake, T. *Polym. J.* **1984**, *16*, 187.
(5) Okahata, Y.; Taguchi, K.; Seki, T. *J. Chem. Soc., Chem. Commun.* **1985**, 1122.
(6) Antonietti, M.; Conrad, J.; Thunemann, A. *Macromolecules* **1994**, *27*, 6007.
(7) Antonietti, M.; Radloff, D.; Wiesner, U.; Spiess, H. W. *Macromol. Chem. Phys.* **1996**, *197*, 2713.
(8) Antonietti, M.; Conrad, J. *Angew. Chem., Int. Ed. Engl.* **1994**, *33*, 1869.
(9) Antonietti, M.; Goltner, G. C. *Angew. Chem., Int. Ed. Engl.* **1997**, *36*, 910.
(10) Pantazis, C. C.; Trikalitis, P. N.; Pomonis, P. J.; Hudson, M. J. *Microporous Mesoporous Mater.* **2003**, *66*, 37.
(11) Pantazis, C. C.; Pomonis, P. J. *Chem. Mater.* **2003**, *15*, 2299.
(12) Pantazis, C. C.; Trikalitis, P. N.; Pomonis, P. J. *J. Phys. Chem. B* **2005**, *109*, 12374.
(13) Beck, J. S.; Vartuli, J. C.; Roth, W. J.; Leonowicz, M. E.; Kresge, C. T.; Schmitt, K. D.; Chu, C. T-W.; Olson, D. H.; Sheppard, E. W.; McCullen, S. B.; Higgins, J. B.; Schlenker, J. L. *J. Am. Chem. Soc.* **1992**, *114*, 10834.
(14) Huo, Q.; Margolese, D. I.; Ciesla, U.; Feng, P.; Gier, T. E.; Sieger, P.; Leon, R.; Petroff, P. M.; Schuth, F.; Stucky, G. D. *Nature* **1994**, *368*, 317.
(15) Huo, Q.; Margolese, D. I.; Ciesla, U.; Demuth, D. K.; Feng, P.; Gier, T. E.; Sieger, P.; Firouzi, A.; Chmelka, B. F.; Schuth, F.; Stucky, G. D. *Chem. Mater.* **1994**, *6*, 1176.

10.1021/cm062878g CCC: $37.00
Published on Web 03/03/2007

method of synthesis is trivial and takes place in one step by a simple titration of an acidified solution of Pac, C_nTAB, and tetraethyl orthosilicate (TEOS), plus a metal salt, if doping with metal oxidic species is wanted. (ii) The same system Pac-C_nTAB can be used for the development of either MCM-41 or SBA materials by simple alternation of surfactant C_{16}TAB to C_{14}TAB. (iii) The introduction of some alkaline cations like Mg and Sr in the system Pac-C_nTAB-TEOS results in the morphogenesis of various highly decorated structures reminiscent of biominerals,[11] while the introduction of some transition metal cations like Co also results in patterns of self-organized nanostructured morphologies.[19]

The most abundant natural acidic polyelectrolytes, analogues to Pac, are the poly(amino acids) poly(L-aspartic acid) (P-L-Asp) and the poly(L-glutamic acid) (P-L-Glu). The abundance of those substances in the natural world has a very specific reason and target: they act as binders of basic cations, mainly Ca(II), either for stabilizing the structure of shells in larvae and other protozoans which are made of calcite $CaCO_3$ crystallites,[20] for destabilizing the development of ice crystallites in the cold water fishes and other organisms,[21−23] or for modifying the development of hydroxyapatite crystallites in living organisms.[24−26]

It seems that the first systematic attempt to study the interaction of such acidic poly(amino acids), P-L-Asp and P-L-Glu, with cationic surfactants C_nTAB ($n = 12-22$) has been made by Munoz-Guerra and co-workers.[27−29] These authors have also proposed a model for the configuration of P-L-Asp-C_nTAB and P-L-Glu-C_nTAB complexes, where the poly(amino acidic) backbones interact with each other and are stabilized via the hydrophobic chains of surfactants species which form crystalline paraffinic phases. Obviously, this model is similar to the one proposed for the interaction between Pac and C_nTAB.[8,9] Furthermore, since the system Pac-C_nTAB provides ordered mesoporous silicate materials with the addition of TEOS,[10−12] it is of interest to examine to what extent the systems P-L-Asp/C_nTAB/TEOS and P-L-Glu/C_nTAB/TEOS might result in similar materials. So, the purpose of this work is to examine the intermediate mesophases and the final mesoporous solids obtained by the above systems.

Table 1. Materials Prepared from P-L-Asp and C_nTAB

sample	XRD phase	d_{100} (nm)
P-L-Asp/C_{14}TAB/7.5	hexagonal	3.45
P-L-Asp/C_{14}TAB/8.5	hexagonal	3.54
P-L-Asp/C_{14}TAB/EtOH/7.5	hexagonal	3.59
P-L-Asp/C_{14}TAB/EtOH/8.5	hexagonal	3.62
P-L-Asp/C_{14}TAB/TEOS/uncal	hexagonal	3.84
P-L-Asp/C_{14}TAB/TEOS/calcin		
P-L-Asp/C_{16}TAB/7.5	hexagonal and layer	3.90 and 3.37−1.69
P-L-Asp/C_{16}TAB/8.5	hexagonal	3.84
P-L-Asp/C_{16}TAB/EtOH/7.5	layer	3.20−1.69
P-L-Asp/C_{16}TAB/EtOH/8.5	hexagonal and layer	3.88 and 3.32−1.69
P-L-Asp/C_{16}TAB/TEOS/uncal	hexagonal	4.13
P-L-Asp/C_{16}TAB/TEOS/calcin	hexagonal	3.81

2. Experimental Section

The synthesis of the materials based on the poly(amino acids) P-L-Asp and P-L-Glu (both from Sigma-Aldrich), the surfactants C_{14}TAB and C_{16}TAB, and TEOS as a source of silica took place as follows: The calculated amounts of P-L-Asp (molecular weight (MW) = 5000−15 000) or P-L-Glu (MW = 3000−15 000) and the surfactant were dissolved in distilled water into a 250 mL beaker. The calculation was such that there was a 1:1 correspondence between the molecules of the surfactant and the carboxyl groups of the poly(amino acids), using their mean MW. The obtained solution was acidified by the addition of 0.1 N HCl to pH 1.5. Then, a slow titration of the acidified solution started with 0.1 N NH_3, using an automatic Radiometer Copenhagen system. The titration was stopped at selected pH values to isolate samples for characterization. The samples obtained and characterized in this way will be designated in the following, for example, as P-L-Asp/C_nTAB/7.5 or P-L-Glu/C_nTAB/8.5, if no silica source was added. The final number corresponds to the pH where the sample was isolated. In some cases a small amount 0.5% of ethanol was added in the hydrolysis bath and the corresponding designation will be P-L-Asp/C_nTAB/EtOH/7.5. When TEOS was added as a silica source in the initial solution, the designation will be, for example, P-L-Asp/C_nTAB/TEOS/6.5. The materials thus prepared, with some of their properties, are shown in Tables 1 and 2 for P-L-Asp/C_nTAB and P-L-Glu/C_nTAB, respectively.

The samples isolated at the chosen pH values during the titration/preparation procedure were dried at room temperature and then characterized by X-ray diffraction (XRD) analysis for their structure, thermogravimetry/differential thermal analysis (TG/DTA) for their thermal stability, scanning electron microscopy (SEM) for their structural features, and circular dichroism (CD) for the conformation of the polypeptide−C_nTAB ($n = 14, 16$) complexes. The XRD experiments took place in a Bruker Advance P8 system using Cu Kα radiation ($l = 1.5418$) with a step size of 0.02° s^{-1}. The nonsilicate samples were put in the instrument's holder in their dried gel form, while the silicates in their powder form after calcination at 600 °C and the removal of organics (see below) were analyzed.

(16) Monnier, A.; Schuth, F.; Huo, Q.; Kumar, D.; Margolese, D.; Maxwell, R. S.; Stucky, G. D.; Krishnamurty, M.; Petroff, P.; Firouzi, A.; Janicke, M.; Chmelka, B. F. *Science* **1993**, *261*, 1299.
(17) Zhao, D.; Feng, J.; Huo, Q.; Melosh, N.; Fredrickson, G. H.; Chmelka, B. F.; Stucky, G. D. *Science* **1998**, *279*, 548.
(18) Zhao, D.; Huo, Q.; Feng, J.; Chmelka, B. F.; B. F.; Stucky, G. D. *J. Am. Chem. Soc.* **1998**, *120*, 6024.
(19) Katsoulidis, A. P.; Petrakis, D. E.; Armatas, G. S.; Trikalitis, P. N.; Pomonis, P. J. *Microporous Mesoporous Mater.* **2006**, *92*, 71.
(20) Mann, S. *Biomineralization*; Oxford University Press: New York, 2001.
(21) Sikes, C. S.; Wierzdiski, A. In *Biomimetic material chemistry*; Mann, S., Ed.; VCH: New York, 1996; pp 249−278.
(22) U.S. Patent 5,942,150. U.S. Patent 6,913,707. U.S. Patent 7,060,199.
(23) U.S. Patent 20050037472.
(24) Lowenstam, H. A.; Weiner, S. *Science* **1985**, *227*, 51.
(25) Nancollas, G. H. In *Biomineralization: chemical and biochemical perspectives*; Mann, S, Webb, J., Williams, R. J. P., Eds.; VCH: Weinheim, 1989; pp 157−187.
(26) Goldberg, H. A.; Warner, K. J.; Li, M. C.; Hunter, G. K. *Connect. Tissue Res.* **2001**, *42*, 25.
(27) Lopez - Carrasquero, L.; Montserrat, S.; Martinez de Ilarduya, A.; Munoz-Guerra, S. *Macromolecules* **1995**, *28*, 5535.
(28) Perez-Camero, G.; Garcia-Alvarez, M.; Martinez de Ilarduya, A.; Fernadez, C.; Campos, L.; Munoz-Guerra, S. *Biomacromolecules* **2004**, *5*, 144.
(29) Garcia-Alvarez, M.; Alvarez, J.; Alla, A.; Martinez de Ilarduya, A.; Herranz, C.; Munoz-Guerra, S. *Macromol. Biosci.* **2005**, *5*, 30.
(30) (a) Beck, J. S.; Vartuli, J. C.; Roth, W. J.; Leonowicz, M. E.; Kresge, C. T.; Schmitt, K. D.; Chu, C. T-W.; Olson, D. H.; Sheppard, E. W.; McCullen, S. B.; Higgins, J. B.; Schlenker, J. L. *J. Am. Chem. Soc.* **1992**, *114*, 10834. (b) Huo, Q.; Margolese, D. I.; Ciesla, U.; Feng, P.; Gier, T. E.; Sieger, P.; Leon, R.; Petroff, P. M.; Schuth, F.; Stucky, G. D. *Nature* **1994**, *368*, 317. (c) Huo, Q.; Margolese, D. I.; Ciesla, Demuth, D. K.; Feng, P.; Gier, T. E.; Sieger, P.; Firouzi, A.; Chmelka, B. F.; Schuth, F.; Stucky, G. D. *Chem. Mater.* **1994**, *6*, 1176.

Table 2. Materials Prepared from P-L-Glu and C_nTAB

sample	XRD phases	d_{100} (nm)
P-L-Glu/C_{14}TAB/7.5	hexagonal	3.60
P-L-Glu/C_{14}TAB/8.5	hexagonal	3.60
P-L-Glu/C_{14}TAB/EtOH/7.5	hexagonal	3.60
P-L-Glu/C_{14}TAB/EtOH/8.5	hexagonal	3.60
P-L-Glu/C_{14}TAB/TEOS/uncal	hexagonal	4.13
P-L-Glu/C_{14}TAB/TEOS/calcin	hexagonal	3.90
P-L-Glu/C_{16}TAB/7.5	hexagonal	4.10
P-L-Glu/C_{16}TAB/8.5	hexagonal	4.10
P-L-Glu/C_{16}TAB/EtOH/7.5	hexagonal	4.10
P-L-Glu/C_{16}TAB/EtOH/8.5	hexagonal	4.10
P-L-Glu/C_{16}TAB/TEOS/uncal	hexagonal	4.31
P-L-Glu/C_{16}TAB/TEOS/calcin	hexagonal	4.13

The thermogravimetric tests took place in a STA 449 C Jupiter system by Netzsch, using air as a flowing gas (20 mL min^{-1}) and α-alumina as a balance. The SEM took place in a Jeol JSM 5600 system operating at 20 kV. The samples before each experiment were exposed to Au vapors for about 60 s, to avoid charge effects by creating a conductive metal film on them. Finally, the CD spectra were recorded at room temperature in a Jasco J-710 spectrophotometer using 0.1 cm path length quartz cell. The spectra were obtained from samples isolated at pH 7.5 and 8.5 which were dissolved in a solution of 100 mL H_2O + 600 mL TFE (trifluoroethanol) + 600 mL CH_3CN.

When TEOS was added into the hydrolysis bath, the dried silicate products obtained were consequently calcined at 600 °C. Those calcined silicate porous solids will be designated in the following as P-L-Asp/C_nTAB/TEOS/6.5/calcin and they are included in Tables 1 and 2 with some of their properties. The porosity of those materials was examined by N_2 adsorption−desorption porosimetry at 77 K in a Sorptomatic 1990 Fisons porosimeter using the BET (Braunauer−Emmett−Teller) methodology. Before each measurement the sample (∼100 mg) was degassed at 150 °C and $P = 10^{-3}$ Torr for 6 h. The results are in Table 3.

3. Results

The method of preparation is based on the gradual neutralization of a strongly acidic solution (pH 1.5), containing the poly(amino acid), the surfactant, and the source of silica, by ammonia solution. Three such typical titration curves in the form pH = *f*(mL of 0.1 N NH_3) and the corresponding typical conductivity curves in the form conductivity = *f*(pH) (i) in the P-L-Asp alone, (ii) after the addition of C_{16}TAB, and finally (iii) for the system P-L-Asp/C_{16}TAB/TEOS are shown in the left-hand side of Figure 1. Similar kinds of titration curves were obtained with the use of the P-L-Glu (not shown here).

The formation of hybridic mesophases is envisaged according to the following reaction:

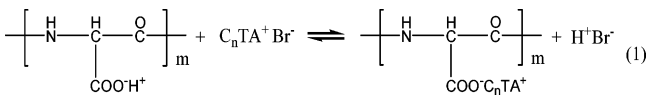

(1)

where *m* is the degree of polymerization of the amino acid.

In strongly acidic conditions the equilibrium shifts to the left, and an unappreciable amount of the poly(L-amino acid)/C_{16}TAB complex is formed. As the pH increases by the addition of NH_3, the equilibrium moves to the right, and gradually a larger amount of organic complex poly(L-amino acid)/C_{16}TAB separates from the solution. An insight into the evolution of the obtained organic complex is provided by the conductivity curves in the right-hand side of Figure 1, namely, P-L-Asp alone, P-L-Asp/C_{16}TAB, and P-L-Asp/C_{16}TAB/TEOS. These curves have similar shapes and bear the blueprint of the titration curve of the poly(L-amino acid) alone, which exhibits two points of zero gradient, one at pH 4, corresponding to the neutralization of the added HCl acid, and a second at pH 8 related to the equilibrium of the reaction:

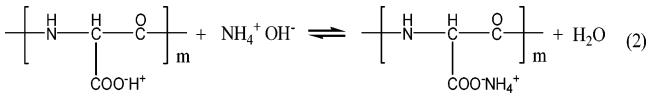

(2)

The other two conductivity curves show similar trends with some important differentiations. The curve of P-L-Asp/C_{16}-TAB shows a point of zero gradient at pH 4 where the complexation according to reaction 1 should start. There is no second point of zero gradient at higher pH, because the poly(amino acid) has, by now, been complexated according to reaction 1, and therefore reaction 2 is not attainable. Nevertheless, it is clear from the curves pH = *f*(mL of 0.1 N NH_3) that a larger amount of NH_3 is now needed to reach the same value of pH, because some of it has been spent to neutralize the produced HBr from reaction 1. The produced $NH_4^+Br^-$ contribute now to the conductivity which is higher by 0.2 (mS cm^{-1}). The addition of TEOS does not affect appreciably the conductivity, which means that the hydrolyzed silicate products (dimers, trimers, tetramers, and cyclic compounds) do not remain free but bound to the hybridic structure.

In Figure 2, the CD spectra of the complexes P-L-Asp/C_{14}TAB and P-L-Glu/C_{14}TAB isolated at pH 7.5 and 8.5 are shown. The solvent was a mixture of 100 mL H_2O + 600 mL TFE + 600 mL CH_3CN.

The XRD patterns of the uncalcined materials P-L-Asp/C_{14}TAB and P-L-Asp/C_{16}TAB isolated at pH values 7.5 and 8.5 are shown in Figure 3 on the left-hand side. In the right-hand side of Figure 3, the XRD patterns of the same samples hydrolyzed/prepared in a bath containing 0.5% EtOH are also shown.

In Figure 4 on the left-hand side the XRD patterns of the uncalcined samples P-L-Glu/C_{14}TAB and P-L-Glu/C_{16}TAB isolated at pH values 7.5 and 8.5 are shown, while at the right-hand side are similar data after the addition of 0.5% EtOH.

Table 3. Specific Surface Areas S_p (m^2 g^{-1}), Pore Volumes V_p (cm^3 g^{-1}), and the Maxima of the psd D_{max} (nm) Estimated According to the Method of Horvath−Kawazoe for the Calcined Silicate Materials

sample	S_p (BET) (m^2 g^{-1})	V_p (cm^3 g^{-1})	D_{max} (nm)	observations from the N_2 adsorption−desorption isotherms
P-L-Asp/C_{14}TAB/TEOS/6.5/calcin	511	0.30		mainly random porosity with extended microporosity
P-L-Asp/C_{16}TAB/TEOS/6.5/calcin	816	0.82	2.63	mainly ordered mesoporosity
P-L-Glu/C_{14}TAB/TEOS/6.5/calcin	1076	0.89	2.46	ordered and random mesoporosity
P-L-Glu/C_{16}TAB/TEOS/6.5/calcin	1001	1.12	2.60	ordered and random mesoporosity

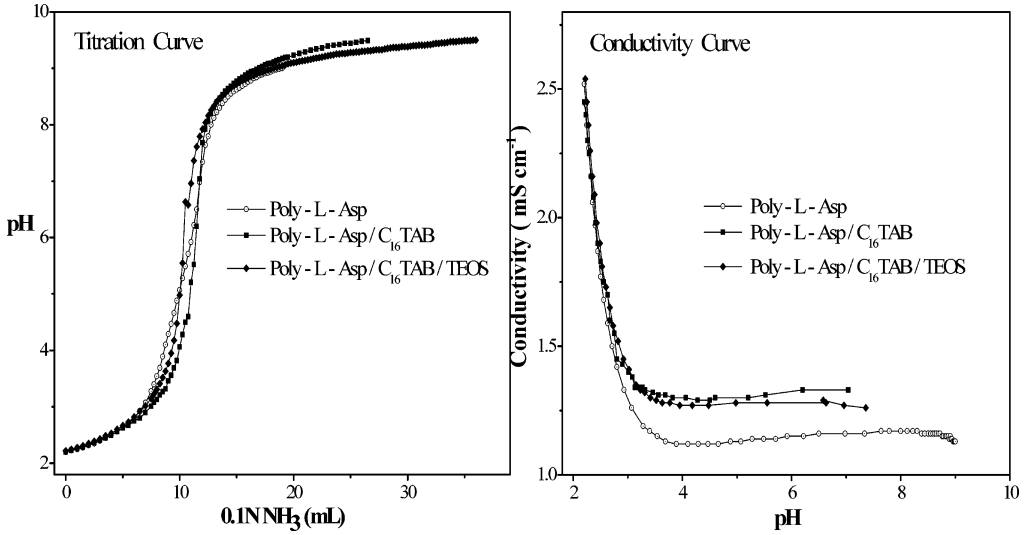

Figure 1. Typical titration curves in the form pH = *f*(mL NH_3) (left) and typical conductivity curves in the form conductivity = *f*(pH) (right) for the P-L-Asp alone, after the addition of C_{16}TAB, and for the system P-L-Asp/C_{16}TAB/TEOS.

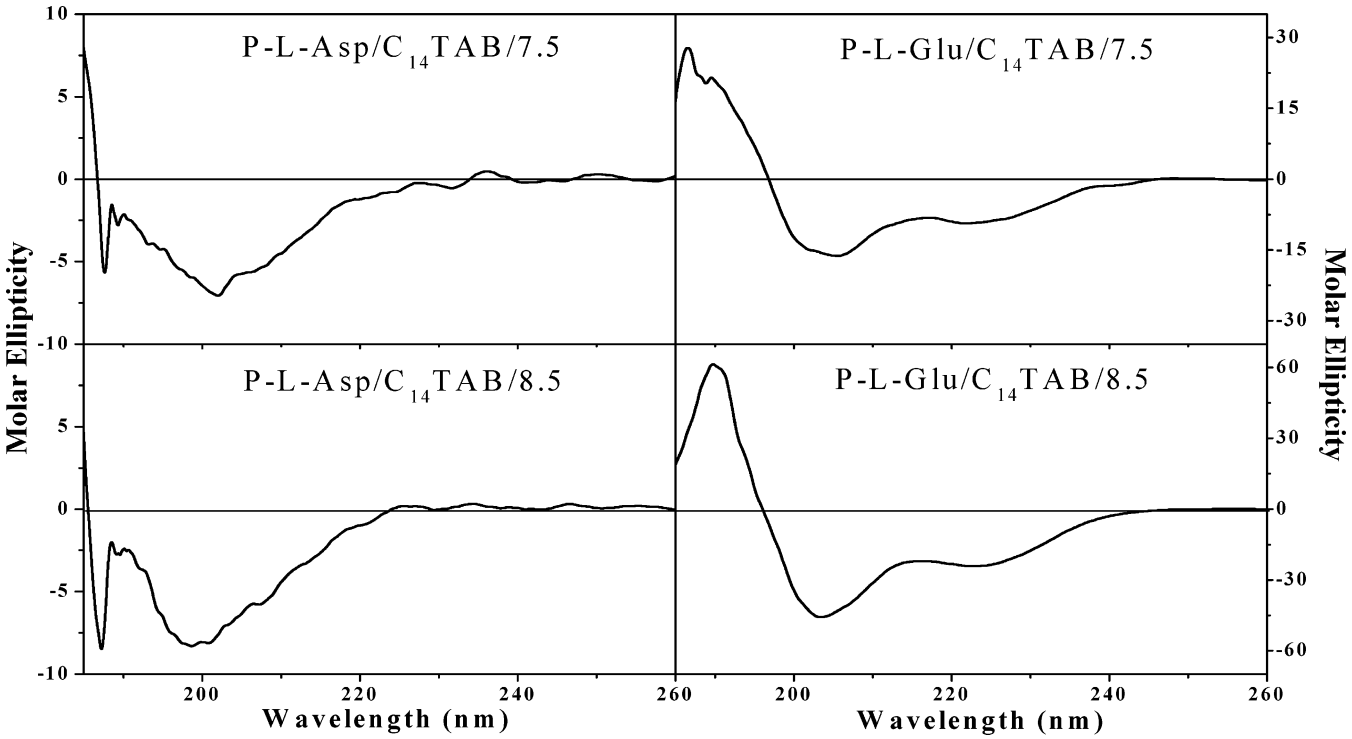

Figure 2. CD spectra of the complexes P-L-Asp/C_{14}TAB (left); P-L-Glu/C_{14}TAB (right) isolated at pH 7.5 (upper part) and 8.5 (lower part) and dissolved in solutions of 100 mL of H_2O/600 mL of TFE/600 mL of CH_3CN.

In Figure 5, the XRD patterns of the silicate *uncalcined* materials, as well as those for the *calcined* samples of P-L-Asp/C_{16}TAB/TEOS and P-L-Glu/C_{16}TAB/TEOS isolated at pH 6.5, are shown

In Figure 6 the TG/DTA signals are shown for the samples P-L-Asp/C_{16}TAB/TEOS and P-L-Glu/C_{16}TAB/TEOS.

In Figures 7 and 8 typical SEM micrographs are shown for all the samples in the form of triplets as follows: The upper micrographs correspond to the dried hybridic phases of poly(amino acid)/C_nTAB; the middle micrographs correspond to the *uncalcined samples* poly(amino acid)/C_nTAB/TEOS; and the lower micrographs correspond to the SEM for the *calcined samples* poly(amino acid)/C_nTAB/TEOS.

Finally, in Figure 9 typical N_2 adsorption−desorption isotherms for the silicate porous materials obtained after calcination of the samples P-L-Asp/C_nTAB/TEOS (n = 14, 16) and P-L-Glu/C_nTAB/TEOS (n = 14, 16) are shown together with the pore size distribution (psd) estimated according to the Horvath−Kawazoe (HK) method.

4. Discussion

The complexes which are formed by the interaction of poly(amino acids) and the surfactants C_nTAB are expected to be typical comb-like structures like those proposed by Munoz-Guerra and co-workers.[27−29] The backbones of the structures are the poly(amino acids). CD spectra of the complexes P-L-Asp/C_{14}TAB (left) and P-L-Glu/C_{14}TAB

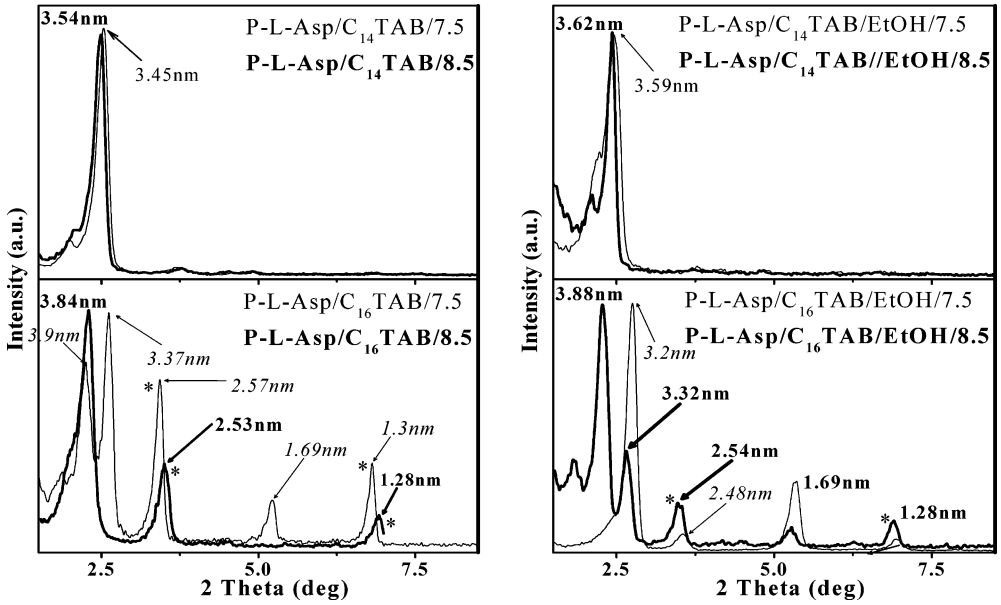

Figure 3. Left part: XRD patterns of the samples P-L-Asp/C_{14}TAB (upper part) and P-L-Asp/C_{16}TAB (lower part) isolated at pH values 7.5 and 8.5. Right part: Similar to those in the left part but with the addition of 0.5% EtOH. The peaks indicated by stars correspond to C_{16}TAB.

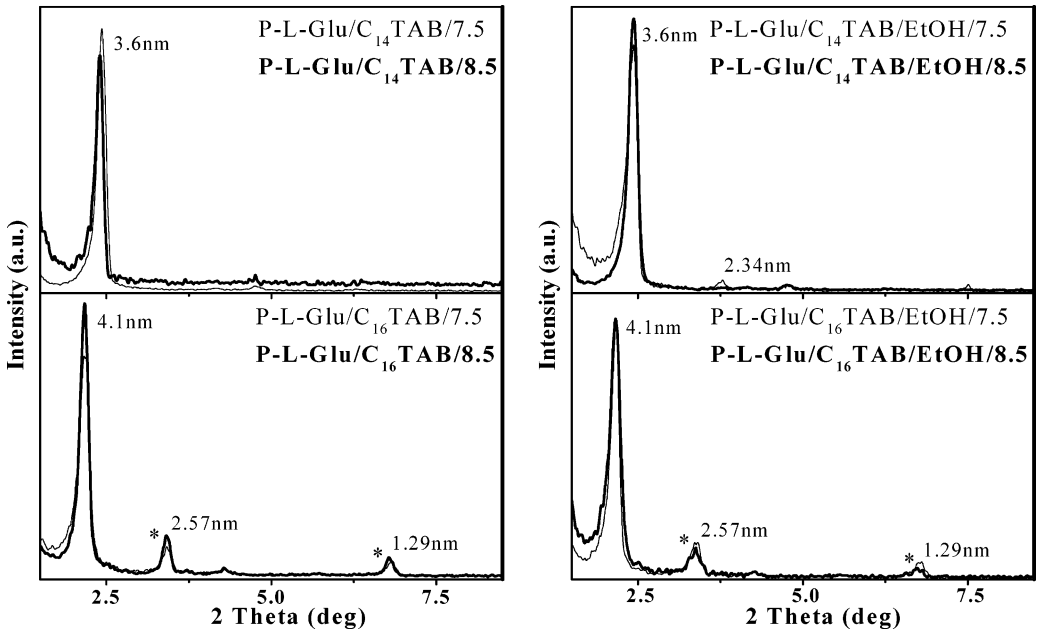

Figure 4. Left part: XRD patterns of the samples P-L-Glu/C_{14}TAB (upper part) and P-L-Glu/C_{16}TAB (lower part) isolated at pH values 7.5 and 8.5. Right part: Similar to those in the left part but with the addition of 0.5% EtOH. The peaks indicated by stars correspond to C_{16}TAB.

(right) are shown in Figure 2. The samples of the latter show distinct features of helicity, that is, a positive band at 192 nm and two negative bands at 205−209 nm and 222−225 nm. The percentage of the secondary structures in both cases was estimated using the CD deconvolution (CDNN program) described by Bohm et al.[31] In the case of P-L-Glu/C_{14}TAB the mesophase was constituted of almost 100% helical structures. It is well-known that the presence of TFE, in such cases, induces the development of helicity because it decreases the interaction of helices with external hydrogen bonds. These helical structures can be α-helix, otherwise 4_{13}-helix, and/or the so-called 3_{10}-helix.[32] The α-helix (or 4_{13}-helix) contains a sequence of four amino acids per turn, and the turns form 13-member rings bridged by internal hydrogen bonds. The 3_{10}-helix contains a sequence of three amino acids per turn, and the turns form 10-member rings bridged by internal hydrogen bonds.[32,33] The percentage of the 3_{10} and 4_{13}-helices can be estimated using the following semi-empirical relationships:[32]

$$\% \, 3_{10}\text{-helix} = 100[\theta_{208}/21\,500]$$

and

$$\% \, \alpha\text{-helix} = 100[(\theta_{222} + 3000)/33\,000]$$

where θ_{208} and θ_{222} correspond to the maxima of the adsorption bands at 208 and 222 nm. Using these semi-empirical fitting relationships, the ratio [% 3_{10}-helix]/

(31) Bohm, G.; Muhr, R.; Jaenicke, R. *Protein Eng.* **1992**, *5*, 191.

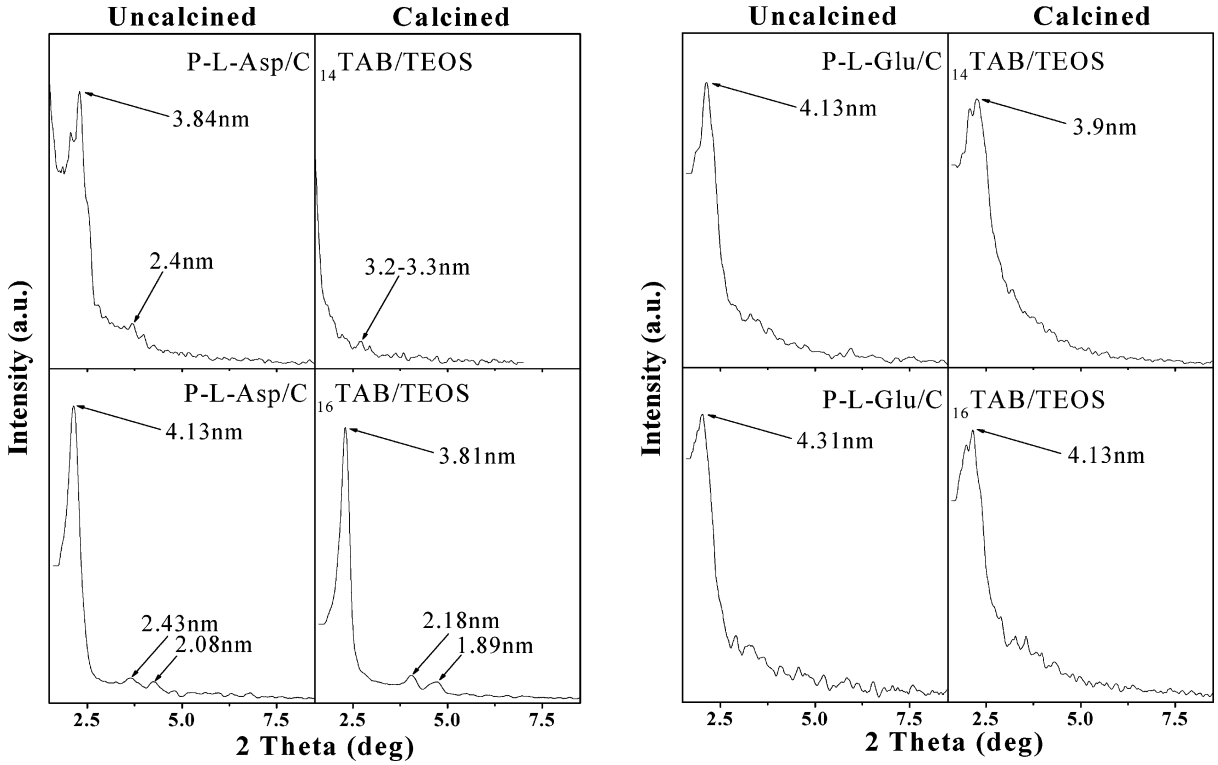

Figure 5. XRD patterns of the silicate materials P-L-Asp/C_{16}TAB/TEOS as well as P-L-Glu/C_{16}TAB/TEOS isolated at pH values 6.5: left, uncalcined samples; right, calcined samples.

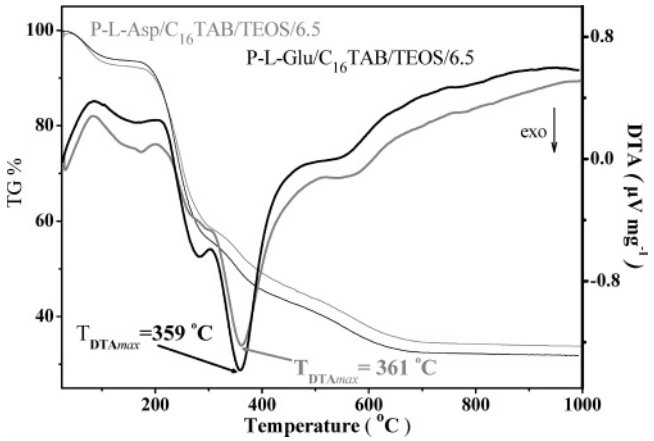

Figure 6. TG and DTA of the samples P-L-Asp/C_{16}TAB/TEOS, as well as of P-L-Glu/C_{16}TAB/TEOS isolated at pH values 6.5.

[% α-helix] was found to be around 70:30 in the case of samples P-L-Glu/C_{14}TAB isolated at both pH 7.5 and 8.5.

Nevertheless, in the case of P-L-Asp/C_{14}TAB the whole structure, always according to the analysis CDNN program, is made up of around 1/3 antiparallel β-sheet, 1/3 β-turn, and 1/3 random coil configurations. In that case, it is not possible to estimate the percentage of particular helices.

So, the presence of Glutamic acid results in mesophases with more ordered characteristics. This is also apparent in the XRD data (Figure 4). On the contrary, the presence of aspartic acid results in a mixture of conformations, that is, 1/3 antiparallel β-sheet, 1/3 β-turn, and 1/3 random coil. In other words, the mesophases contain heterogeneous and disordered components. This situation is also reflected in the

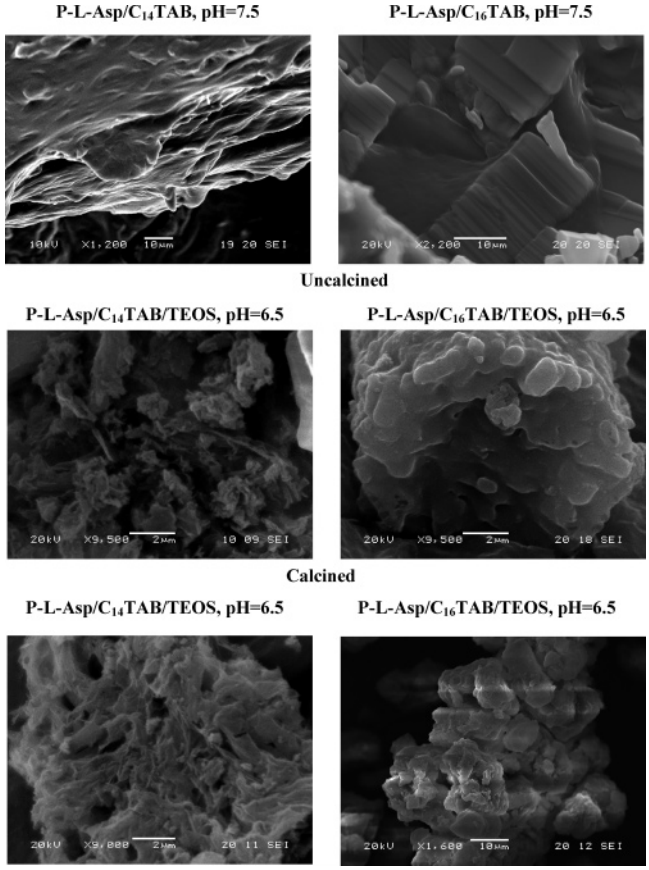

Figure 7. Left part: Typical SEM micrographs for the samples P-L-Asp/C_{14}TAB (top); P-L-Asp/C_{14}TAB/TEOS/uncalcined (middle), and P-L-Asp/C_{14}TAB/TEOS/calcined (bottom). Right part: As in the left part but for C_{16}TAB instead of C_{14}TAB.

(32) Haynes, S. R.; Hagius, S. D.; Juban, M. M.; Elzer, P. H.; Hammer, R. P. *Peptide Res.* **2005**, *66*, 333.
(33) Krikorian, D.; Panou-Pomonis, E.; Voitharou, C.; Sakarellos, C.; Sakarellou-Daitsiotou, M. *Bioconjugate Chem.* **2005**, *16*, 812.

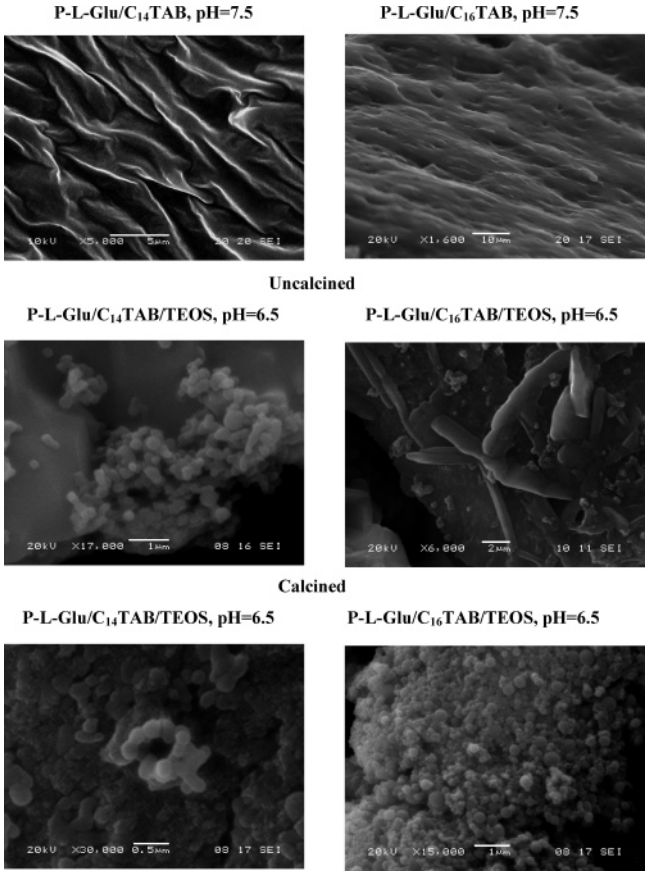

Figure 8. Left part: Typical SEM micrographs for the samples P-L-Glu/C_{14}TAB (top); P-L-Glu/C_{14}TAB/TEOS/uncalcined (middle), and P-L-Glu/C_{14}TAB/TEOS/calcined (bottom). Right part: As in the left part but for C_{16}TAB instead of C_{14}TAB.

XRD spectra (Figure 3). The ellipticity of the samples containing glutamic acid is higher because this amino acid is an inherent strong inducer of helices, as shown by Chou and Fasman some time ago.[34]

The formed micellar aggregates are organized spontaneously in a closed packed hexagonal structure in the case of P-L-Glu, independently of the surfactant employed, C_{14}TAB or C_{16}TAB, the pH of isolation of the sample, 7.5 and 8.5, or the presence of small amounts of ethanol, as it can be easily verified by the XRD results in Figure 4, which are also summarized in Table 2. The inter-backbone distance is 3.60 nm in the case of the system P-L-Glu/C_{14}TAB and increases by 0.5 to 4.1 nm in the system P-L-Glu/C_{16}TAB for obvious reasons.

For the samples based on P-L-Asp, the complexation with C_{14}TAB leads to mesophases similar to those described above for the P-L-Glu with the difference that the distance between the micellar aggregates tends to be somehow lower by almost 0.1−0.2 nm, as a result of the shorter side chain of aspartic acid compared to that of glutamic acid. A distinct difference with the above cases appears in the samples P-L-Asp/C_{16}TAB. In this case the micellar aggregates tend to self-organize in two phases, one the usual hexagonal closed packing MCM-41 type structure, plus a layer structure as seen in the XRD results in Figure 3, which are summarized in Table 1. Namely, the P-L-Asp/C_{16}TAB/7.5 sample possesses a hexagonal structure with inter-micellar distance at 3.90 nm plus a layer structure with interlamellar distance at 3.37 nm. When the pH increases to 8.5 the whole structure is switched to hexagonal. The addition of 0.5% of EtOH results in the transformation of the P-L-Asp/C_{16}TAB/7.5 sample to a totally layered structure and of P-L-Asp/C_{16}TAB/EtOH/8.5 partly to a hexagonal and to a layered one. The interlamellar structures are well-organized as seen by the double reflections, the main around 3.2−3.3 nm and the second-order reflections at 1.69 nm. It is suggested that the two structures are transformed to each other by folding of the layered micellar aggregates to cylindrical ones and vice versa.

The inorganic silicate materials obtained after the calcination of the hybridic samples P-L-Asp/C_{16}TAB/TEOS/6.5 and P-L-Glu/C_{16}TAB/TEOS/6.5 show clearly in XRD ordered porosity similar to that observed in the well-known MCM-41 materials,[30] as seen in the XRD spectra in Figure 5. The distance between the centers of the pores is around 4.0 nm, which is practically similar to the analogous structures obtained by the system Pac/C_{16}TAB[10−12] instead of poly(amino acids)/C_{16}TAB. This leads to the conclusion that the mechanism of development of micelles is similar in both cases.

The distance 4.13 nm observed between the mesopores of silicate material, obtained after calcination at 600 °C of the sample P-L-Glu/C_{16}TAB/TEOS/6.5 (Figure 5), is less than the distance of 4.31 nm for the uncalcined sample. The shrinking should be due to the removal of organics. As it can be seen in Figure 6, at this temperature the organic part has practically been removed from the hybridic sample and only the inorganic phase remains which accounts for the 35−37% of the original mass. Assuming in a schematic way that the hybridic material is built up of units of the form *X*[Si−O]−*Y*[−CO−NH−CH−CH_2−CH_2−OCO−ATC_{16}], it can be easily verified that *X*:*Y* should obtain values around 4.0−4.5, in other words about four to five layers of [Si−O] units cover each micelle. The formation of such micellar aggregates could be imagined along the following reaction path.

$$4(\text{Si-[OEt]}_4) + 16\text{H}_2\text{O} + [-\text{CO}-\text{NH}-\text{CH}-\text{CH}_2-\text{CH}_2-\text{OCO}-\text{ATC}_{16}] \rightarrow 4\text{Si(OH)}_4-[-\text{CO}-\text{NH}-\text{CH}-\text{CH}_2-\text{CH}_2-\text{OCO}-\text{ATC}_{16}] + 16\text{EtOH} \quad (3)$$

It should be kept in mind that the above reaction 3 is schematic and does not include the condensation of the hydro silicate species or the sites on which they are attached on the soft organic backbone, a problem unsolved for the moment. Nevertheless, if two hybridic micellar aggregates are in contact to each other, the combined silicate wall/shell should be about 8−10 [Si−O] units thick, corresponding to 10−12 nm as observed experimentally in usual MCM materials.[10−12]

The SEM micrographs of the hybridic samples P-L-Asp/C_{14}TAB/7.5 and P-L-Asp/C_{16}TAB/7.5 are in the upper part of Figure 7, while of the hybridic samples P-L-Glu/C_{14}TAB/7.5 and P-L-Glu/C_{16}TAB/7.5 are in the upper part of Figure

(34) (a) Chou, P. Y.; Fasman, G. P. *Biochemistry* **1974**, *13*, 211; (b) **1974**, *13*, 222.

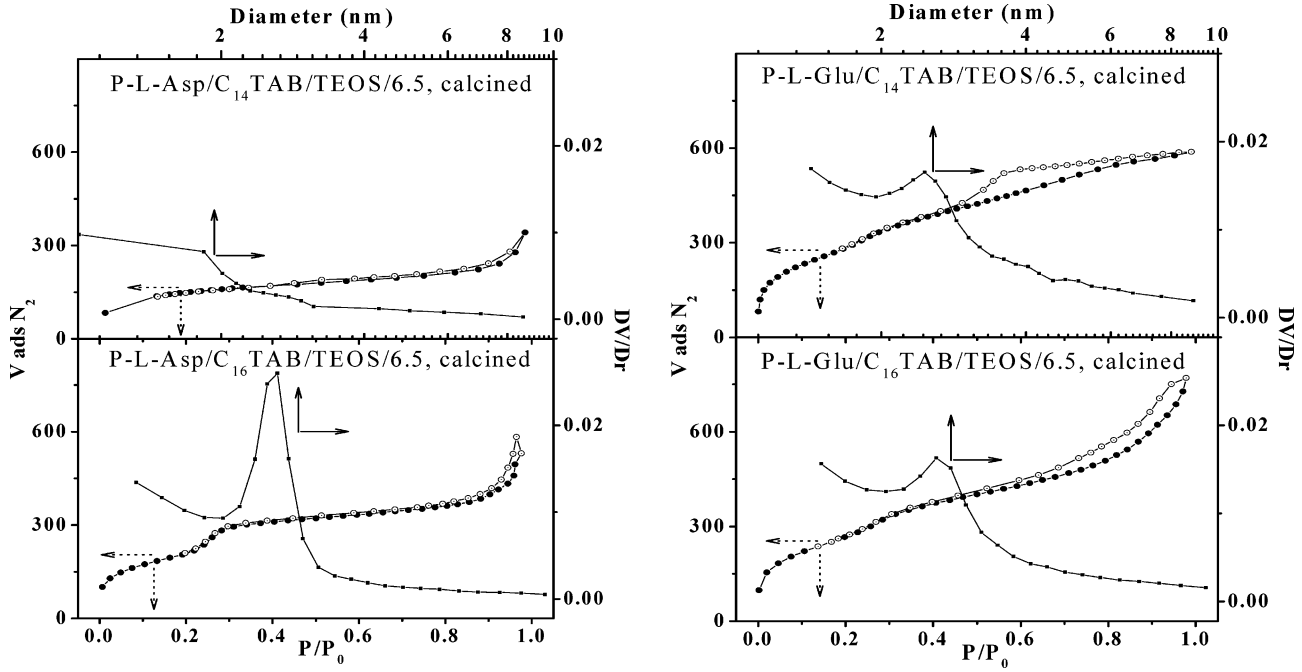

Figure 9. Left Part: N_2 adsorption−desorption isotherms for the calcined samples P-L-Asp/C_{14}TAB/TEOS/6.5 (upper part) and P-L-Asp/C_{16}TAB/TEOS/6.5 (lower part) and the corresponding psd estimated according to the Horvath−Kawazoe method. Right part: As in the left part but for P-L-Glu instead of P-L-Asp.

8. In all cases, the whole optical field appears as a corrugated sheet, but the wrinkles apparent on the surface have more or less parallel directions. This anisotropic development of wrinkles in the corrugated hybridic sheet should be directed by the backbone of the structure which is the poly(L-amino acids) bridged with the C_nTAB surfactants groups. There are various knots, shallow cavities, and heterogeneities on this anisotropically wrinkled/corrugated hybridic sheet, which reflect the imperfections of the structure due to various reasons, for example, loops of the backbones and gaps in the matching between the surfactants groups. Those heterogeneities are less profound in the case of hybridic samples containing glutamic acid, compared to the ones with aspartic acid. This is in line with the fact that the last provides less ordered structures in the XRD results (compare Figure 3 containing aspartic acid to Figure 4 containing glutamic acid). It is also worthwhile to mention that for the sample P-L-Asp/C_{16}TAB/7.5, the image normal to the sheet reveals a layered structure (see upper left image in Figure 7). The layers in this figure have thickness between 30 and 300 nm. This is in line with the XRD results in Figure 3 that refer to the same sample, which indicates clearly a layered configuration, as discussed above.

The SEM micrographs of the uncalcined samples P-L-Asp/C_{14}TAB/TEOS/6.5 and P-L-Asp/C_{16}TAB/TEOS/6.5 are in the middle part of Figure 7 and of the uncalcined samples P-L-Glu/C_{14}TAB/TEOS/6.5 and P-L-Glu/C_{16}TAB/TEOS/6.5 in the middle part of Figure 8. Careful observation reveals that the samples based on C_{14}TAB tend to be more irregular, while the ones based on C_{16}TAB tend to form some kind of tiny slabs sometimes developed to scaly structures (P-L-Asp/C_{16}TAB/TEOS/6.5) or to peculiar wrinkles, not parallel any more, but crossing each other or starting from a common point (P-L-Glu/C_{16}TAB/TEOS/6.5).

Eventually, the final silicate products obtained after the calcination of the above mesophases are in the lower parts of Figures 7 and 8. Those silicate materials are practically amorphous.

From the N_2 adsorption−desorption isotherms of the calcined samples P-L-Asp/C_{14}TAB/TEOS/6.5/calcin and P-L-Asp/C_{16}TAB/TEOS/6.5/calcin (upper and lower parts of the left-hand part of Figure 9, respectively), as well as of the samples P-L-Glu/C_{14}TAB/TEOS/6.5/calcin and P-L-Glu/C_{16}-TAB/TEOS/6.5/calcin (as previously but in the right part of Figure 9), the specific surface areas S_p (m^2 g^{-1}) were estimated according to the BET methodology. The corresponding values are in Table 3 together with the pore volumes V_p (cm^3 g^{-1}) and the maximum of the psd (D_{max}, pore diameter) estimated according to the method of Horvath−Kawazoe. The development of the silicate mesoporous materials from the corresponding mesophases is envisaged to take place according to the schematic path shown in Figure 10.

The shape of the isotherm for P-L-Asp/C_{14}TAB/TEOS/6.5/calcin indicates that this sample possesses mainly random porosity (upper-left-hand part of Figure 9) in the micropore range, as presumed from the psd. This is in line with the XRD data (see Table 1 and Figure 5) which do not show any ordered Bragg reflections. The surface area is around 511 m^2 g^{-1}. On the contrary, the sample P-L-Asp/C_{16}TAB/TEOS/6.5/calcin (lower left part of Figure 9) shows much higher surface area around 816 m^2 g^{-1} and ordered porosity in line with the XRD data in Figure 5. The psd shows a narrow maximum of pore diameters at 2.63 nm which should be compared with the value of 3.81 nm found by XRD: The difference 1.18 nm corresponds to the thickness of the silicate walls.

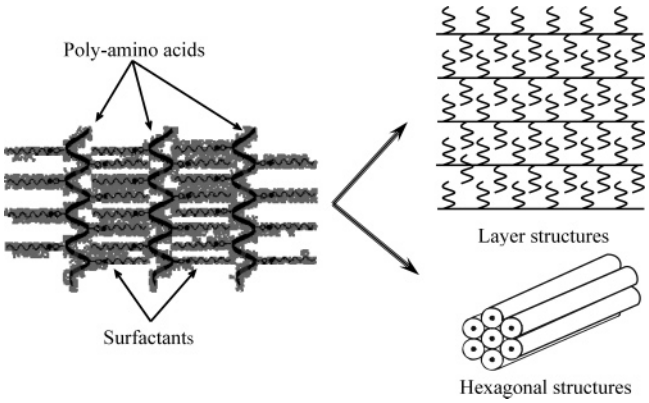

Figure 10. Comb-like ionic complexes of P-L-Asp and P-L-Glu with the surfactants C_nTAB (left), which led either to layer structures or to cylindrical micelles with hexagonal symmetry and eventually to MCM-41 type silicate materials (right).

The isotherms for the samples P-L-Glu/C_{14}TAB/TEOS/6.5/calcin and P-L-Glu/C_{16}TAB/TEOS/6.5/calcin (right part of Figure 9) show mixed ordered and random mesoporosity. Indeed, although the XRD data in Figure 5 show Bragg reflections at 3.90 and 4.13 nm, respectively, those reflections are wide and weak, meaning that only small amounts of the sample possess ordered porosity. This is corroborated by the fact that the corresponding psd in Figure 9, although in the mesopore region, is much wider compared to the best case of P-L-Asp/C_{16}TAB/TEOS/6.5/calcin discussed above.

5. Conclusions

In this work it has been shown that it is possible to develop structurally hierarchical micellar aggregates using as a backbone poly(amino acids), like P-L-Asp and P-L-Glu. On the acidic side chains of those polyelectrolytes, cationic surfactants such as C_nTAB (n = 14, 16) can be bound. Finally on the external surface of such organic hybridic entities a thin silicate shell can be formed via hydrolysis of a proper source of silica, like TEOS. These mesophases may yield after calcination mesoporous silicate materials with ordered porosity. To the best of our knowledge this is the first time such hybridic phases have been used for the development of mesoporous silicate materials.

The precursor mesophases are complex and can be manipulated by the kind of self-organized species participating in their development, especially the kind of poly(amino acid) and the kind of surfactant. Samples based on P-L-Glu and C_{14}TAB tend to provide more ordered and less complex systems.

Acknowledgment. We acknowledge financial support to E.K.K. from the program PENED 2003 of the GSRT, as well as technical support by the facilities XRD, SEM, and TG/DTG/DSC of the Ring of Laboratories of the University of Ioannina. Various parts of this work were also assisted by the programs PYTHAGORAS financed by EU and the Ministry of Education in the context of the Project EPEAEK.

CM062878G